



Vertical and lateral flux on the continental slope off Pakistan: correlation of sediment core and trap results

H. Schulz^{1,*} and U. von Rad^{2,*}

¹Fachbereich für Geowissenschaften, Paleobiology, University of Tübingen, Hölderlinstr. 12, 72074 Tübingen, Germany

²Rosenstraße 19c, 30916 Isernhagen, Germany

*formerly at: Bundesanstalt für Geowissenschaften und Rohstoffe (BGR), PF 510153, 30631 Hannover, Germany

Correspondence to: H. Schulz (hartmut.schulz@uni-tuebingen.de)

Received: 13 May 2013 – Published in Biogeosciences Discuss.: 23 July 2013

Revised: 27 March 2014 – Accepted: 12 April 2014 – Published: 16 June 2014

Abstract. Due to the lack of bioturbation, the varve-laminated muds from the oxygen minimum zone (OMZ) off Pakistan provide a unique opportunity to precisely determine the vertical and lateral sediment fluxes in the nearshore part of the northeastern Arabian Sea. West of Karachi (Hab area), the results of two sediment trap stations (EPT and WPT) were correlated with 16 short sediment cores on a depth transect crossing the OMZ. The top of a distinct, either reddish- or light-gray silt layer, ²¹⁰Pb-dated as AD 1905 ± 10, was used as an isochronous stratigraphic marker bed to calculate sediment accumulation rates. In one core, the red and gray layer were separated by a few (5–10) thin laminae. According to our varve model, this contributes < 10 years to the dating uncertainty, assuming that the different layers are almost synchronous. We directly compared the accumulation rates with the flux rates from the sediment traps that collected the settling material within the water column above. All traps on the steep Makran continental slope show exceptionally high, pulsed winter fluxes of up to 5000 mg m⁻² d⁻¹. Based on core results, the flux at the seafloor amounts to 4000 mg m⁻² d⁻¹ and agrees remarkably well with the bulk winter flux of material, as well as with the flux of the individual bulk components of organic carbon, calcium carbonate and opal. However, due to the extreme mass of remobilized matter, the high winter flux events exceeded the capacity of the shallow traps. Based on our comparisons, we argue that high-flux events must occur regularly during winter within the upper OMZ off Pakistan to explain the high accumulations rates. These show distribution patterns that are a negative function of water depth and distance from the shelf. Some of the sediment fractions show marked shifts in ac-

cumulation rates near the lower boundary of the OMZ. For instance, the flux of benthic foraminifera is lowered but stable below ~ 1200–1300 m. However, flux and sedimentation in the upper eastern Makran area are dominated by the large amount of laterally advected fine-grained material and by the pulsed nature of the resuspension events at the upper margin during winter.

1 Introduction

About 1 million km³ of shelf and slope waters of the global ocean are found to be permanently hypoxic, with more than half of that volume in the Indian Ocean (Helly and Levin, 2004). After the pioneering study of von Stackelberg (1972) on the sedimentation along the Indian–Pakistan margin of the northern Arabian Sea, numerous campaigns and initiatives revealed the key role of the organic-rich, laminated sediments in studying the linkages between the production, pathways and preservation of marine organic matter under low bottom-water oxygen conditions (Paropkari et al., 1992; Pedersen et al., 1992; Calvert et al., 1995; Cowie et al., 1999; Keil and Cowie, 1999; van der Weijden et al., 1999; von Rad et al., 1999; Schulte et al., 2000; Suthhof et al., 2000; Cowie, 2005; Wiggert et al., 2005; Cowie and Levin, 2009).

The northern Arabian Sea off Pakistan is characterized by a stable, distinct oxygen minimum zone (OMZ) between water depths of 200 m and about 1200 m that impinges on the continental slope. The very low oxygen concentrations at intermediate depths (< 0.2 mL L⁻¹) result from low ventilation and from oxygen consumption by microbial

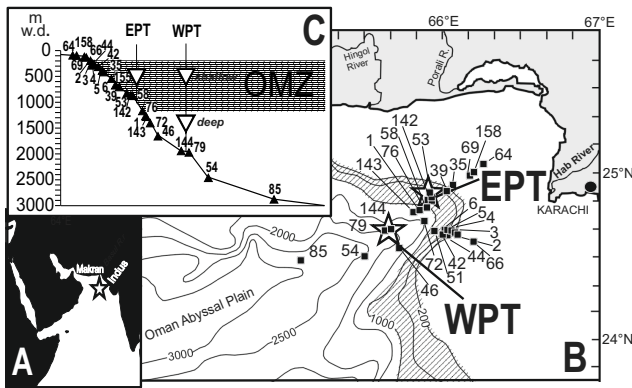


Figure 1. Investigation area in the northwestern Indian Ocean off Pakistan. (A) Arabian Sea with Makran and Indus continental margins. (B) Position of sediment trap deployments and sediment stations (“Hab area” W of the Hab river) from two oceanographic cruises, *SONNE* 90 (numbers 35 onward) and *METEOR* 32/2 (numbers 1–6). Most sites are distributed below the narrow Makran shelf to the northeast and some down the broader Indus margin to the southeast. (C) Idealized transect “Hab transect” of sediment stations between 92 and 2881 m with sediment traps EPT and WPT. Distance between traps is ~ 20 km. Stippled area is the oxygen minimum zone, OMZ.

decomposition of organic matter within the water column and on the seafloor. High surface water primary productivity and organic matter flux is triggered by the strength and direction of the seasonally reversing summer (southwest) and winter (northeast) monsoonal circulation, and may also depend on fluvial and eolian terrigenous input (Sirocko and Sarin, 1989; Ramaswamy et al., 1991). Vertical fluxes in the open oceanic environment in the western Arabian Sea were intensely studied by means of time series of moored and drifting sediment traps (Haake et al., 1993; Nair et al., 1989; Rixen et al., 1999; Pollehne et al., 1993). In contrast, our knowledge on the scales and seasonal timings of the marine biogenic and terrigenous fluxes on the steep margin zones of the northern Arabian Sea is still fragmentary.

The sediments along the continental slope off Pakistan (Fig. 1a) are characterized by a distinct lamination due to suppressed bioturbation (von Stackelberg, 1972). However, the hypoxic bottom water conditions preventing the sediment from being mixed by burrowing organisms may be only one important factor for the preservation of laminae. Exceptionally high sedimentation of more than 1 mm per year, linked to the high lateral fluxes of remobilized terrigenous and marine matter, was observed off the active, steep Makran margin off western Pakistan (Schulz et al., 1996; Andruleit et al., 2000; Lückge et al., 2002; Schulz et al., 2002; von Rad et al., 2002a, b). Thus, high fluxes and sediment redistribution may also contribute to the preservation of sediment lamination. However, comparable laminations are not observed off India, where slope sedimentation rates can be as high, nor are they off Oman, where slopes are also steep (Paropkari et al.,

1992). But sediment laminations are also found off the Indus Delta, where sedimentation rates are lower and the slope is less steep (Cowie et al., 1999). From sedimentary models of varve formation and from simple mass calculations, we may expect a significant contribution of fine-grained, remobilized matter to the steep continental slope from the narrow shelf areas nearby. This adds also to the particle flux derived from local biological productivity and thus complicates the identification of the sediment sources and processes. Also, MODIS satellite images show examples of distinct sediment plumes extending from the coastal zone offshore (Bourget et al., 2010). These plumes might also contribute to the formation of the winter sediment laminae.

The cores from the steep Hab area west of Karachi (Fig. 1b) host the most distinct sediment laminae on millimeter to sub-millimeter scales (von Rad et al., 1999; 2002b). The distinct nature of the varved sediments along the steep Makran is dominated by a high fraction of lithic components. For at least the past 5000 years, there has been a continuous deposition of annual laminae couplets, which point to a strong seasonality in the amount and composition of material settling to the seafloor (von Rad et al., 1999). Microscopic analyses of thin sections show distinct alternations of dark-colored, organic-carbon-rich and light-colored, organic-carbon-poor terrigenous laminae, which suggest a cyclic pattern due to changes in the flux and composition during summer and winter (Berger and von Rad, 2002; Lückge et al., 2002). Cores from the less steep Indus Pakistan margin, situated to the southeast and distant from the Makran, are characterized by a more regular pattern in lamina thickness.

Quantitative flux estimates are needed to better describe the complex sedimentation processes in the water column and on the seafloor at the continental margin off Pakistan. However, direct observations of the summer and winter situations are missing to corroborate the formation of the sediment laminae and the transfer of sediments to the deep sea. Four sediment trap moorings in eastern Pakistan (EPT) and western Pakistan (WPT) (Fig. 1) have been deployed within and below the OMZ off Pakistan. However, the flux estimates from these traps were only fragmentary and showed strong, unexpected temporal and spatial variability. None of the four traps in 1993/1994 and 1995/1996 sampled the full year as planned. All traps stopped collecting in the winter season, three of four traps presumably due to a huge flux of matter remobilized on the upper margin (von Rad et al., 1995; Andruleit et al., 2000; Schulz et al., 2002; von Rad et al., 2002b). The reason for these flux events recorded in the traps and their role in the sedimentation off Pakistan is poorly constrained.

In the present study, we focus on the quantification of sediments accumulated along a depth transect in the Hab area (Fig. 1) between ~ 200 and ~ 2000 m water depth, and directly compare these accumulation rates with the limited numbers of flux estimates derived from sediment traps deployed in the overlying water column. Published estimates of

surface water productivity can be used to quantitatively better describe the local flux of organic carbon at a certain depth derived from primary production (Sarnthein et al., 1992). However, this approach may not be valid in the near-coastal environment, where lateral fluxes are high and may be temporally dominant. To better determine their role, we will focus on possible differences in the amount and preservation of bulk fractions of biogenic and mineral matter found above, in the center and below the OMZ. The concentration and accumulation of the major sand-sized components preserved along our core transect across the OMZ will be used to provide additional information.

2 Geologic setting and previous geological investigations

The study area on the continental margin of Pakistan in the northeastern Arabian Sea represents a restricted area between the narrow active Makran margin to the northwest and the Indus margin to the southeast (Fig. 1a), where the broad shelf is typical for the passive Indian margin (Fig. 1a).

The “Hab area” (Fig. 1b) is characterized by the three tectono-sedimentologic settings: (1) to the north the accretionary complex covered by thick uplifted wedges and sediment prisms that is part of the steep Makran margin (stations 39, 53), (2) a lower accretionary wedge zone with rather regular topography on vertical scales of some 100 m (stations 1, 35, 58–158) and (3) a more gentle NE slope of the Murray Ridge to the southeast that was formed by large blocks of slumped sediments (stations 2–6, 42–46, 54). The Hab area is drained by deep, mostly ENE–WSW-trending channels.

In the near-surface sections of 16 box cores and 6 multicores, up to 12 cm thick reddish- or gray-whitish-colored silty-clay layers were identified (Staubwasser and Sirocko, 2001). Based on the strong visual contrast of both layer types to the over- and underlying laminated sediment (Fig. 2), these thick layers can be traced over large overlapping areas, possibly covering some 1000 and 600 km², respectively. Most cores show either the red or the gray-whitish layer. The red layer is found more on the Makran side, to the north of the ENE–WSW-trending channels. All laminated *SONNE* cores (except station 35 at 416 m) showed a distinct reddish-colored silt layer that can be regarded as a silt turbidite, sometimes with fining upward or indistinct internal laminations (Schulz et al., 1996). In contrast, the gray-whitish layer is observed more to the southeast on the Indus side, at shallower depths (stations 2–6; see also supplementary online material), but not at all sites: cores 44 KG and 42 KG are more similar to the Makran cores (Staubwasser and Sirocko, 2001). In core 58 KG (Fig. 2d) presumably both types of layers were found, with the reddish-colored layer (~13–22 cm) above the whitish one (~22.5–25.5 cm). The whitish layer is separated from the red layer by 5–10 thin sediment laminae. The two types of fine-grained clastic sediment appear to be

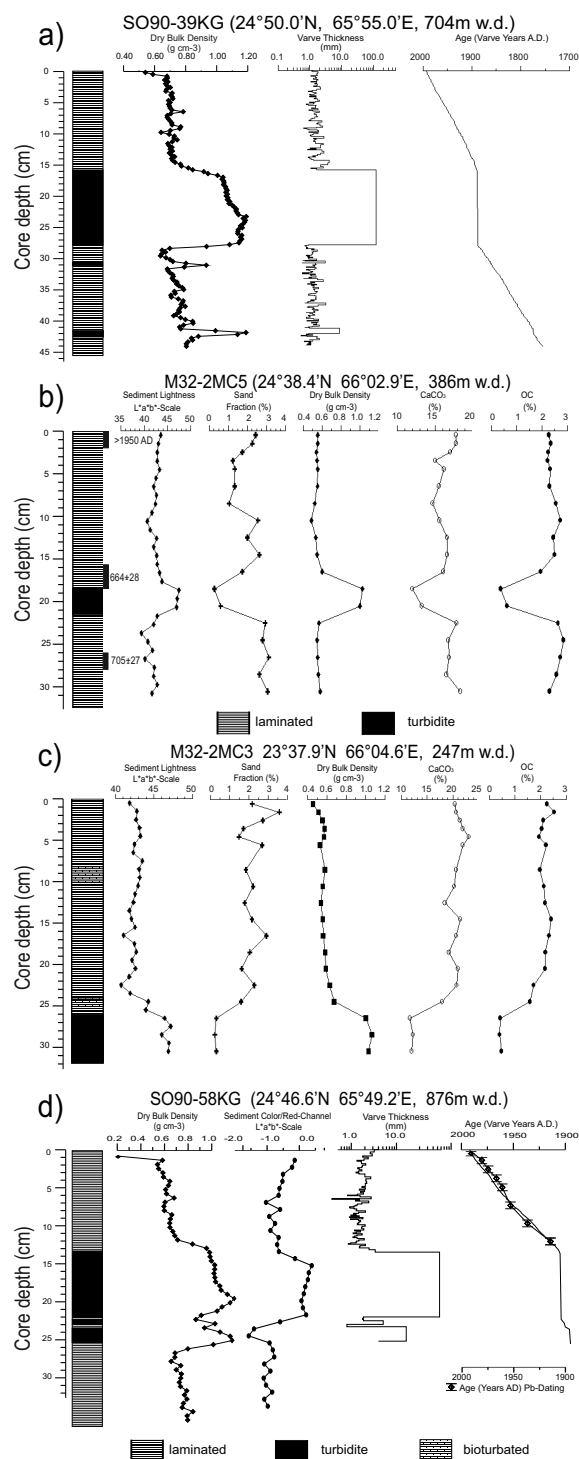


Figure 2. Examples from four short sediment cores along the Pakistan margin for high-resolution analyses of sediment properties and dating. Various properties display marked changes because of a 4 to 10 cm thick reddish-gray turbidite deposit. Profiles from the OMZ show distinct sediment laminations as well. According to models of their formation, varve counts, ²¹⁰Pb- and ¹⁴C dating provide a coherent age of AD 1905–1888 for that layer.

very similar in their elemental ratios, as well as in their bulk organic carbon and calcium carbonate contents (Staubwasser and Sirocko, 2001, unpublished data). The type of reddish-colored sediment also occurs in up to a few centimeter-thick intervals in the longer piston and long box cores of the area, interpreted to represent an episodic redeposition of fluvial matter from the Indus shelf, possibly linked to strong rainfall or floods in the hinterland (Schulz et al., 1996; von Rad et al., 2002a). Staubwasser and Sirocko (2001) investigated the light-gray clastic sediment in more detail and concluded that these might consist of material expelled by mud volcanoes from the active Makran margin. In contrast von Rad et al. (2002a) argued that the distinct light-gray to whitish layers are explained as “plume deposits” transporting mud-charged suspensions across the narrow shelf to the slope.

No additional, similarly thick layers are observed further downcore in the longer Holocene records from the Hab area. By establishing the stratigraphic position of the turbidite and plume sedimentation events, the unique event layers, interbedded between laminated sediment, could be ideally used as stratigraphic marker beds for correlation of the short cores. The described layers were sampled again by *SONNE* cruise 130 in the Hab area by the following box cores (KG) and multicores (MC): 268 MC, 605 m; 276 KG, 780 m; 262 MC, 875 m; and 291 MC, 902 m water depth. In cores 262 MC and 291 MC from the same area as 58 KG, the red and whitish layers were found on top of each other again, questioning their exact synchronism.

3 Material and methods

3.1 Sediments and accumulation rates

Twenty box cores (KG) and 6 multicores (MC) (short gravity cores of ~10–50 cm length) were taken in 1993 during *SONNE* cruise SO 90 and in 1995 during *ME-TEOR* cruise M32/2, respectively, and recovered undisturbed top sediments from water depths between 96 and 2881 m. The organic carbon (OC), calcium carbonate (CaCO₃) and opal concentrations were determined following Dietrich and Marchig (1995) and Suthhof et al. (2000). The composition of the coarse fraction larger than 150 microns (μm) in core top samples was counted from a few milliliters of freeze-dried sediment of the top centimeter washed through a 63 μm mesh. The residue was dried at 60 °C and sieved into sub-fractions of 63–150, 150–200, 200–250, 250–315, 315–400 and >400 μm, respectively. Splits of at least 70 grains from the fractions >150 μm were obtained with an Otto microsplitter for each sample. In these splits all grains were identified following the categories (1) inorganic compounds (Inorg.: quartz, mica, oxides, lithic grains), (2) megafossils (Megaf.: sponge spicules, ophiurid remains, pteropods, fish debris, etc.), (3) siliceous tests (Silic.: large radiolarians, diatoms, silicoflagellates), (4) planktic foraminiferal debris

(P.F. debris), (5) intact planktic foraminiferal tests (P.F.) and (6) benthic foraminifera (B.F.). The six categories represent more than 95 % of the >150 μm size fraction. They were used to better characterize the texture and composition of the surface sediment and to identify possible remobilization of sand-sized particles across the steep margin. For example, potential disturbances of the fluffy top layer could be deduced from coarse fractions. Increased numbers of the lithic fractions would indicate mass flows or sediment winnowing. Further, calcite dissolution or corrosion at certain depth may be identified by an increased fragmentation of planktic foraminiferal shells.

Profiles of sediment γ -ray attenuation were analyzed at 0.5 cm intervals using a GEOTECH-multisensor core logger (Schultheiß and Weaver, 1992). Discrete samples were taken at 1–2.5 cm intervals by 10 cm³ syringes or from sliced sediment profiles in order to determine the sediment physical properties of natural water content as well as wet and dry bulk density. The latter two were used to calibrate the parallel profiles of γ -ray attenuation that vary as a function of sediment density (Weber et al., 1997). Using these calibrations from selected cores, a homogenous set of dry bulk density data was generated for 15 sediment profiles of 12 to 40 cm length from water depths of 250 to 1970 m. The 30 cm long multicore MC2 from a depth of 197 m was only described visually prior to discrete sampling, and showed a homogenous light-colored layer of silty clay between 18.0 and 21.0 cm core depth.

A detailed varve chronology was developed for the laminated sediments from the Pakistan margin (Schulz et al., 1996; von Rad et al., 1999). This chronology is based on the assumption that a couplet of one light-gray-colored (winter) lamina plus one dark-gray, organic-rich (summer) lamina was deposited in one year. This assumption was verified by the observation that five light–dark couplets of laminae were accumulated at the upper Makran slope in between 1993 (*SONNE* 90) and 1998 (*SONNE* 130). Lückge et al. (2002) interpreted the thicker light-colored laminae as representing recurrent suspension events linked to high winter precipitation, and the dark-colored laminae as caused by the high summer productivity during the SW monsoon.

About 150 samples from the top 20 cm of laminated sediment at 1 cm intervals of cores MC1, MC3, MC5 and 39 KG, 58 KG were used for ²¹⁰Pb dating to precisely determine the sedimentation rates during the last 150 years. These data are presented here only for core 58 KG (Erlenkeuser, unpublished data). The relative error for the past 1000 years is better than 10 % for that method. Analytical details of the ²¹⁰Pb method are outlined in Erlenkeuser and Peterstad (1984). AMS¹⁴C ages of monospecific samples of *Globigerinoides ruber* (white) or of mixed P.F. were determined at the Leibniz Labor Kiel, Germany.

In order to obtain a quantitative measure on the flux of individual particles and compounds to the seafloor, accumulation rates (ARs) were determined for the 16 short cores,

based on the sedimentation rate estimates from the cores and from the dry bulk densities, following Thiede et al. (1982):

$$AR_{\text{bulk sediment}} = SR p_{\text{dry}}, \quad (1)$$

with AR in $\text{g cm}^{-2} \text{ kyr}^{-1}$, SR in cm kyr^{-1} , and p_{dry} (dry bulk density) in g cm^{-3} .

The accumulation rate of individual compounds, or of the individual sediment components in a sample, is calculated as follows:

$$AR_{\text{component}} = SR p_{\text{dry}} C / 100, \quad (2)$$

where C is the concentration of a compound in percent, and N is the number of the specimens per gram of dry sediment.

3.2 Sediment traps

Four trap moorings of type MARK 7G-21 (McLane Research Laboratories Inc.) at sites EPT ($24^{\circ}45.4' \text{ N}$, $65^{\circ}48.7' \text{ E}$) and WPT ($24^{\circ}35.9' \text{ N}$, $65^{\circ}35.3' \text{ E}$; 2004 m seafloor depth) had been deployed within and below the OMZ off Pakistan (Fig. 1). Collection time was programmed as October 1993 to February 1994 and May 1995 to February 1996 (EPT2). Sampling intervals for the 28 cups used in the present study were 22 days for WPT and EPT1 and 24 days for EPT2, respectively (Table 2). Prior to deployment, cups were treated with mercuric chloride. The total mass fluxes, CaCO_3 and lithogenic particle fluxes were also presented in Andrulleit et al. (2000) and in Schulz et al. (2002), who studied the coccolithophore and planktic foraminiferal fluxes, and by Treppke, who studied the diatoms (von Rad et al., 2002b, their Fig. 11). Details of trap and sample preparation, OC, CaCO_3 , biogenic opal analyses, and of the derivation of fluxes are described in Haake et al. (1993), Andrulleit et al. (2000) and Suthhof et al. (2000). The mass accumulation rates were previously used by Suthhof et al. (2000).

All flux and accumulation rate results are listed in Table 2. Estimates of local primary productivity were adopted from Antoine et al. (1996). The accumulation rate for the respective sediment property was derived from that analysis of the core top sample 0–1 cm. The density value for a particular station was averaged from the measurements above the marker layer (Fig. 3). Similarly, sedimentation rates were calculated assuming a linear accumulation process of the laminated/bioturbated sediments over the past ~ 100 years. Most estimates for the study are expressed as $\text{mg m}^{-2} \text{ d}^{-1}$ or specimens (= spec.) $\text{m}^{-2} \text{ d}^{-1}$ to allow for direct comparison.

4 Results

4.1 A turbidite or turbid top layer as stratigraphic marker for core correlation

Staubwasser and Sirocko (2001) presented sedimentological and geochemical data on the distinct, up to 12 cm thick reddish turbidite they observed in nearly all *SONNE* cores of the

Hab area. An investigation of the *METEOR* short multicores, overlapping with the *SONNE* sediments, shows in some cases that *METEOR* cores 1–6 are thinner, having a gray to light-gray silty layer at 10 to 24 cm depth (see supplementary on-line material). The cores 2–6 were taken from a channel, while cores 42 and 44 KG were recovered from the nearby flank of that channel on the NE slope of the Murray Ridge, (Fig. 1b). We show that both types of layers display internal structures that can be best seen in their high-resolution profiles of dry bulk density (Fig. 2b, d). We observe faint grading in the reddish-colored, decimeter-thick beds in some *SONNE* cores, as well as highest density at their bottoms (Fig. 3), that might reflect coarser grain sizes or compaction at the base of these layers. The density profile of shallow core 44 KG suggests that the thick layers might also display more internal structure reflecting at least two sublayers. From a slight increase in sand content near the base, faint regular grading can also be traced in the relatively thin, light-gray layer of core MC5 (Fig. 2b).

All cores display high sediment densities for the layer of ≥ 0.8 (Fig. 3) corresponding to low OC content of $< 1\%$ (Fig. 2). Few pelagic microfossils, grading and rapid flow expansion leading to variable thicknesses are typical diagnostic features of that type of fine-grained silt turbidite (Piper and Stow, 1991). However, quality of the extremely soft *METEOR* cores is poor compared to the *SONNE* box cores, where most of these criteria can be observed. Due to increasing bottom water oxygen at depths above and below the OMZ supporting macrofaunal bioturbation, the marker could not be determined with precision outside the OMZ. The upper boundary of that marker layer is still feasible as a slight relative increase in density in the high-resolution logs below the OMZ down to 1970 m (Fig. 3). Although the sedimentation at the central Makran is characterized by the deposition of up to some millimeter- to decimeter-thick light-colored “turbid layers” (von Stackelberg, 1972) and by larger turbidites (Schulz et al., 1996, von Rad et al., 2002b; Bourget et al., 2010), no other thick red and/or light-gray whitish layer was found in the upper meters of cores in the Hab area. Assuming that the reddish and light-gray to whitish layers reflect different sedimentation events, we are able to estimate the level of uncertainty from assuming that the layers are diachronous. In 58 KG (and also in cores *SONNE* 130–262 MC and 291 MC), the reddish turbidite is separated from that whitish layer immediately below by thin, alternating black and olive-gray laminae. According to our varve model, these 5–10 millimeter-thick layers would correspond to less than 10 years (Fig. 2d; see X-ray figure of Staubwasser and Sirocko, 2001).

4.2 Local sedimentation rates by Pb dating, varve chronology and ^{14}C ages

Counting of the varves in various cores, including replicate runs, yielded an age of AD 1888 and AD 1905 in 39 KG

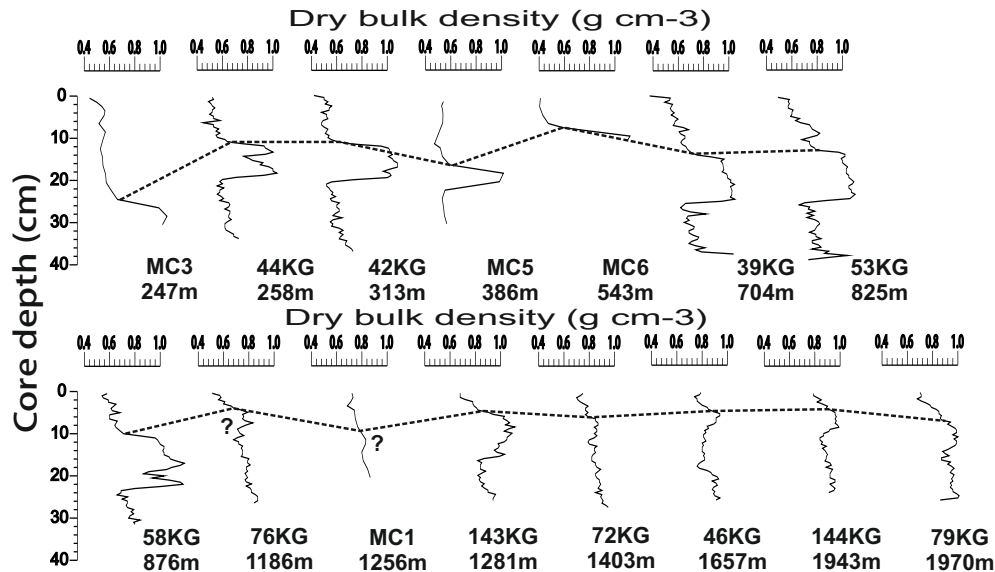


Figure 3. Correlation of short box (KG) and multicores (MC) by means of their sediment density (here expressed as dry bulk density) profiles above and below the silt turbidite, used for correlation (stippled line). A sudden increase in density with depth (in centimeters) is evident for the laminated cores within the OMZ. Density is lowest near the core top and increases with depth by compaction. Below OMZ depths, this boundary is smoothed by bioturbation, becoming more faint with water depth and distance from the shelf.

and 58 KG, respectively (Fig. 2a, d). ^{210}Pb dating of core 58 KG and of other short sediment profiles indicates that the younger date of AD 1905 (i.e., about 90 years before 1993/1996) may be more reliable. The error of that data amounts to not more than 10 %, which conforms to ± 10 years. The sedimentation rate (SR) has a strong impact on the respective accumulation rates (ARs) (see Eq. 1), as changes in dry bulk density are relatively small, and in general show similar trends with very low values near the core top. The 13 density profiles show a rather uniform density maximum for the marker turbidite used for the correlation. Density profiles from above that layer show values increasing with water depth. Most profiles for the past ~ 100 –500 years from OMZ depths show values of $< 0.6 \text{ g cm}^{-3}$ with a major shift at $\sim 1200 \text{ m}$ (compare 76 KG and MC1, Fig. 3) to densities of $> 0.7 \text{ g cm}^{-3}$.

The date of AD 1905 suggests sedimentation rates of 167 cm kyr^{-1} and 150 cm kyr^{-1} for the two core profiles, whereas by the correlation via the marker horizon, sedimentation rates at shallow depth are distinctly higher (up to 272 cm kyr^{-1}). At greater depth and more distant from the coast, sedimentation rates were lower (46 KG and 144 KG, 44 cm kyr^{-1}) (Table 2). Sedimentation rates of $\geq \sim 200 \text{ cm kyr}^{-1}$ on the shelf (MC2, MC3) are in line with Limmer et al. (2012), who determined a sedimentation rate of 195 cm kyr^{-1} in the core Indus-10 on the inner shelf at 71 m, to the east of the Hab area. In order to support our stratigraphic models, the AMS ^{14}C ages from intervals from above and further below the clay-silt layer in cores M32–MC1 and M32–MC5 show a difference of 40 ^{14}C years over

the interval of 7.3 cm in the latter core. The suggested sedimentation rate for that interval is $\sim 180 \text{ cm kyr}^{-1}$.

Further, the ages of the laminated intervals can be used to assess the radiocarbon age of the local surface water. This “reservoir effect” of the ocean water is known to be highly variable in space and time. As expected, the planktic foraminiferal ^{14}C dates of the top sediments of MC1 and MC5 yielded negative ages caused by the post-bomb high atmospheric radiocarbon concentrations (Table 1). In contrast, the three laminated intervals in cores MC1 and MC5 yielded uncorrected, “conventional” ^{14}C ages of 747 ± 27 , 664 ± 25 , and 705 ± 23 years, respectively, that correspond to varve ages of AD 1820, AD 1903, and AD 1867. From the difference between the varve ages of 175 years, 92 years and 128 years of these depth intervals (which clearly predate the spike of “bomb” radiocarbon in 1964), and the corresponding “conventional” ^{14}C ages, we could determine essentially uniform reservoir ages of 582, 572 and 577 years from the three different ^{14}C dates. The average reservoir age of 577 years is different from the 640 years used by von Rad et al. (1999).

4.3 Sedimentation patterns

4.3.1 Bulk and sand fraction analysis across the OMZ

The sediments on the continental margin off the coast of Pakistan can be described as organic-rich, carbonaceous silty clays with typically 1–4 % OC content and 15–30 % CaCO_3 , with deposits on the Makran slope having slightly lower OC of 1–2.5 % and higher CaCO_3 of ~ 20 % on average than at

Table 1. List of AMS ^{14}C dates from latest Holocene laminated sediments of the oxygen minimum zone (OMZ) off Pakistan.

Lab number	Sample	Corrected pMC	Conventional age (yr)	Varve age (yr)*	Reservoir age (yr)
KIA201	M32-2MC1, 0–5 cm	100.42 ± 0.33	> AD 1950	1970	–
KIA202	M32-2MC1, 18.5–22.5 cm	91.12 ± 0.31	747 + 27 / –27 BP	1820	582
KIA773	M32-2MC5, 0–2.5 cm	105.05 ± 0.41	> AD 1950	1984	–
KIA774	M32-2MC5, 15–18.5 cm	92.06 ± 0.32	664 + 28 / –28 BP	1903	572
KIA775	M32-2 MC5, 26–28 cm	91.59 ± 0.30	705 + 27 / –27 BP	1867	577

*assuming constant sedimentation rates (Table 2).

comparable depth on the Indus slope. An exception is the carbonate-rich facies of relict sands on the shelf, which contain a significant component of biogenic calcite and a bulk carbonate content of up to 70 % (von Stackelberg, 1972). These carbonate sands are restricted to shallow water depths of < 200 m on the Makran side, but are found down to 400 m below present sea level on the Indus side. The shallow sites (Fig. 1c) are situated within a relatively flat channel morphology. Above the OMZ the flat shelf may provide space and substrate for sessile and vagile CaCO_3 -producing organisms, which is in line with the high relative abundance and AR of megafossils at < 250 m water depth (Fig. 4). Below that depth, the sand fraction decreases to only 0.5–3.0 wt% (Fig. 2), where most of the coarse fraction is of planktic and benthic foraminiferal tests with a few hundred to a few thousand spec. g^{-1} .

Remarkable for OMZ sediments is the high abundance of benthic foraminifers (Fig. 4). Based on accumulation rates, we can say that the benthic foraminiferal population at the lower OMZ boundary and below shows stable but low numbers (~ 10 – 50 spec. $\text{m}^{-2} \text{yr}^{-1}$), while benthic foraminifera clearly are more important within the OMZ (~ 500 – 1000 spec. $\text{m}^{-2} \text{yr}^{-1}$). The accumulation of benthic foraminiferal shells is highest in the shallow waters, with a maximum AR of 4000 spec. $\text{m}^{-2} \text{yr}^{-1}$ on the shelf outside the OMZ. The minimum in the benthic foraminifera frequencies found at the lower OMZ boundary is in contrast to a maximum in relative abundance of planktic foraminifera, the latter group making up to 80 % of the sand fraction. We note also an increase in the AR of planktic foraminifera and planktic foraminiferal debris, thus causing the dilution effect on the benthic foraminifera. In contrast to other high-productivity areas, siliceous microfossils (diatoms, radiolarians, silicoflagellates, sponge spicules) are rare in the sand fraction of the surface sediments. In general, the abundance and relative frequencies of siliceous tests in the coarse fraction increase with depth; however no clear pattern is seen, possibly because of the low numbers of less than 100 spec. g^{-1} .

The accumulation of inorganic particles can be interpreted mostly as precipitates of small oxides/oxihydroxides (Law et al., 2009) at the lower OMZ. Pyrite was found sporadically

inside the spherical tests of the planktic foraminifer *Orbulina universa*.

4.3.2 High accumulation rates of bulk sediment fractions

A general decrease of SRs, and hence ARs, is observed with increasing water depth. Individual stations at the shelf edge show a large variability with the highest AR of bulk sediment of > 4000 $\text{mg m}^{-2} \text{d}^{-1}$ (Fig. 5a). In contrast, the two sites 42 KG and 44 KG immediately below display only half of that flux. MC5 shows a slightly higher AR bulk of 2600 $\text{mg m}^{-2} \text{d}^{-1}$. On the shelf, ARs are highest and show largest variability. MC6 (543 m, Fig. 1) from the same region is the uppermost core on the slope and displays a relatively low AR bulk of 1110 $\text{mg m}^{-2} \text{d}^{-1}$ (Table 2).

The deeper sites (e.g., 39 KG) are situated on the Makran side of the Hab transect. Also, these sites show, in general, a decrease of AR bulk, with a decline with water depth and distance from the shelf from > 2700 to ~ 1100 $\text{mg m}^{-2} \text{d}^{-1}$ (Fig. 5a). The negative trend is typical for all bulk components (Fig. 5b, c) except for the sediment concentration of OC (Fig. 5d) that is distinctly lowered at the uppermost sites at the Indus side of the investigated Hab transect. In contrast, CaCO_3 has very high relative and absolute accumulation rates on the shelf, where its relative fraction is about 25 %. At greater depths, that fraction decreases to less than 15 %.

4.3.3 High-flux events (HFEs) during winter caused incomplete trap time series

The longest trap series (EPT2; see Table 2) collected from late spring (May 1995) to late winter, but stopped abruptly in February 1996. An extremely high bulk particle flux of 2000 to > 5000 $\text{mg m}^{-2} \text{d}^{-1}$ was also measured two years before, in early 1994, in shallow traps EPT1 and WPTs (Fig. 6). WPTd (1470 m) of the same period had the shortest collection period of less than three months, between October 1993 and mid-January 1994 (Table 2). WPTd apparently was not directly affected by the extreme flux during winter. Collection stopped, although no increase in flux is noticed for that trap.

Table 2. List of fluxes of lithic matter, calcium carbonate (CaCO₃), and organic carbon (OC) in the water column (sediment traps EPT1, EPT2, WPTs and WPTd) and reconstructed accumulation rates (ARs) at the seafloor for 16 short cores at water depths between 196 and 1970 m.

(a) Water column particle flux and composition													
Trap	Trap depth (m)	Sampling start	Sampling end	Sampling (d)	Total flux (mg m ⁻² d ⁻¹)	Lith. flux (mg m ⁻² d ⁻¹)	CaCO ₃ flux (mg m ⁻² d ⁻¹)	Opal flux (mg m ⁻² d ⁻¹)	OC flux (mg m ⁻² d ⁻¹)	Lith. (%)	CaCO ₃ (%)	Opal (%)	OC (%)
EPT1-01	590	15/10/93	05/11/93	22	504	282	108	45	38	55.96	21.5	8.9	7.56
EPT1-02	590	06/11/93	27/11/93	22	680	464	138	43	19	68.28	20.3	6.3	2.84
EPT1-03	590	28/11/93	19/12/93	22	1086	769	164	73	45	70.77	15.1	6.8	4.11
EPT1-04	590	20/12/93	10/01/94	22	4848	3621	713	351	91	74.68	14.7	7.2	1.87
EPT1-05	590	11/01/94	01/02/94	22	4298	3234	639	297	71	75.25	14.9	6.9	1.65
EPT1-06	590	02/02/94	23/02/94	22	3501	2609	523	256	63	74.53	14.9	7.3	1.80
EPT2-01	590	05/05/95	29/05/95	24	1678	1081	404	111	45	64.45	24.1	6.6	2.70
EPT2-02	590	30/05/95	23/06/95	24	501	326	96	42	21	65.07	19.1	8.3	4.20
EPT2-03	590	24/06/95	18/07/95	24	688	484	109	51	24	70.43	15.8	7.5	3.50
EPT2-04	590	19/07/95	12/08/95	24	188	126	32	15	8	67.05	17.2	8.2	4.20
EPT2-05	590	13/08/95	06/09/95	24	1337	1012	148	107	39	75.67	11.1	8.0	2.91
EPT2-06	590	07/09/95	01/10/95	24	2444	1841	225	226	84	75.34	9.2	9.3	3.44
EPT2-07	590	02/10/95	26/10/95	24	160	106	25	12	9	66.11	15.6	7.8	5.83
EPT2-08	590	27/10/95	20/11/95	24	142	90	26	10	9	63.30	18.5	7.2	6.16
EPT2-09	590	21/11/95	15/12/95	24	136	88	24	9	8	65.15	17.7	6.6	5.90
EPT2-10	590	16/12/95	09/01/96	24	276	190	44	20	12	68.78	16.0	7.2	4.43
EPT2-11	590	10/01/96	03/02/96	24	4296	3270	598	269	89	76.11	13.9	6.3	2.06
EPT2-12	590	04/02/96	28/02/96	24	4077	3124	530	281	79	76.63	13.0	6.9	1.93
WPTS1-01	534	15/10/93	05/11/93	22	213	116	57	18	13	54.32	26.5	8.4	5.94
WPTS1-02	534	06/11/93	27/11/93	22	528	362	97	33	21	68.43	18.3	6.2	3.89
WPTS1-03	534	28/11/93	19/12/93	22	413	230	103	39	23	55.61	25.0	9.5	5.50
WPTS1-04	534	20/12/93	10/01/94	22	1424	994	224	127	44	69.79	15.7	9.0	3.09
WPTS1-05	534	11/01/94	01/02/94	22	5105	3870	738	334	90	75.82	14.4	6.5	1.77
WPTS1-06	534	02/02/94	23/02/94	22	1564	1094	258	143	38	69.95	16.5	9.1	2.46
WPTD1-01	1466	15/10/93	05/11/93	22	353	205	74	39	20	58.18	20.9	10.9	5.57
WPTD1-02	1466	06/11/93	27/11/93	22	485	332	84	37	18	68.48	17.3	7.7	3.62
WPTD1-03	1466	28/11/93	19/12/93	22	471	292	94	46	22	61.90	19.9	9.7	4.69
WPTD1-04	1466	20/12/93	10/01/94	22	199	119	45	21	8	59.53	22.5	10.7	4.02
(b) Seafloor sediment accumulation rates and composition.													
Cruise	Core	Latitude	Longitude	Water depth (m)	Bulk AR (mg m ⁻² d ⁻¹)	Lith. AR (mg m ⁻² d ⁻¹)	CaCO ₃ AR (mg m ⁻² d ⁻¹)	Opal AR (mg m ⁻² d ⁻¹)	OC AR (mg m ⁻² d ⁻¹)	Lith. (%)	CaCO ₃ * (%)	Opal* (%)	OC* (%)
METEOR 32/2	MC2	24°N 37.9'	66°E 06.4'	196	4090	2703	1178	167	75	66.08	28.1	4.0	1.79
METEOR 32/2	MC3	24°N 37.9'	66°E 04.6'	247	4178	1930	910	201	92	72.46	20.8	4.6	2.11
SONNE 90	44 KG	24°N 37.0'	66°E 01.5'	258	2093	1563	396	112	48	74.69	18.0	5.1	2.20
SONNE 90	42 KG	24°N 36.5'	65°E 59.0'	313	2096	1611	351	101	55	76.85	16.0	4.6	2.53
METEOR 32/2	MC5	24°N 38.4'	66°E 02.9'	386	2663	2036	454	137	66	76.46	16.3	4.9	2.37
METEOR 32/2	MC6	24°N 39.2'	66°E 01.0'	543	1053	832	175	55	28	78.99	14.3	4.5	2.25
SONNE 90	39 KG	24°N 50.0'	65°E 55.0'	704	2740	2252	318	159	38	82.20	11.0	5.5	1.31
SONNE 90	53 KG	24°N 48.6'	65°E 55.0'	825	2611	2133	328	129	44	81.71	12.0	4.7	1.61
SONNE 90	58 KG	24°N 46.6'	65°E 49.2'	876	2630	2142	332	141	40	81.44	12.0	5.1	1.44
SONNE 90	76 KG	24°N 40.6'	65°E 41.2'	1168	912	751	115	45	9	82.27	12.0	4.7	0.99
METEOR 32/2	MC1	24°N 44.8'	65°E 46.6'	1266	2047	1678	250	94	31	82.00	12.0	4.5	1.50
SONNE 90	143 KG	24°N 45.0'	65°E 44.3'	1281	1156	946	146	63	12	81.84	12.0	5.2	0.95
SONNE 90	72 KG	24°N 39.1'	65°E 45.4'	1403	1370	1110	187	73	13	81.03	13.0	5.1	0.88
SONNE 90	46 KG	24°N 33.2'	65°E 41.8'	1657	926	1120	117	53	8	81.74	12.0	5.4	0.86
SONNE 90	144 KG	24°N 36.4'	65°E 35.1'	1943	1022	846	119	56	11	82.78	11.0	5.2	0.98
SONNE 90	79 KG	24°N 36.0'	65°E 35.1'	1970	1663	1378	193	96	11	82.89	11.0	5.5	0.60
(b) ff.													
Core	Water depth (m)	Local SR (cm ka ⁻¹)	Inorg. AR (spec. m ⁻² d ⁻¹)	Megafl. AR (spec. m ⁻² d ⁻¹)	Silic. AR (spec. m ⁻² d ⁻¹)	PF-Frag. AR (spec. m ⁻² d ⁻¹)	P.F. AR (spec. m ⁻² d ⁻¹)	B.F. AR (spec. m ⁻² d ⁻¹)	PP** (mg m ⁻² d ⁻¹)	O ₂ -BW*** (mg L ⁻¹)			
MC2	196	205	74	10.470	4	33	1137	4434	711	0.08			
MC3	247	272	8	3033	63	42	806	3681	711	0.07			
44 KG	258	139	4	92	2	21	347	1082	709	0.07			
42 KG	313	144	13	281	4	6	358	1025	708	0.08			
MC5	386	183	0	152	21	8	535	927	714	0.06			
MC6	543	100	0	43	11	18	281	815	716	0.05			
39 KG	704	167	3	79	25	14	258	471	758	0.07			
53 KG	825	144	5	42	5	10	272	329	753	0.07			
58 KG	876	150	3	21	34	37	650	1323	739	0.11			
76 KG	1168	56	1	2	4	52	267	38	717	0.19			
MC1	1266	100	2	16	23	68	158	100	731	0.37			
143 KG	1281	56	0	2	8	7	73	8	730	0.38			
72 KG	1403	67	3	15	4	22	74	27	714	1.36			
46 KG	1657	44	0	2	1	1	13	15	697	1.60			
144 KG	1943	44	3	4	10	7	38	35	706	1.97			
79 KG	1970	78	0	0	12	3	63	47	706	1.99			

*Suthhof et al., 2000.

**Primary productivity PP (Antoine et al., 1996).

***Bottom water oxygen O₂-BW (von Rad et al., 1995).

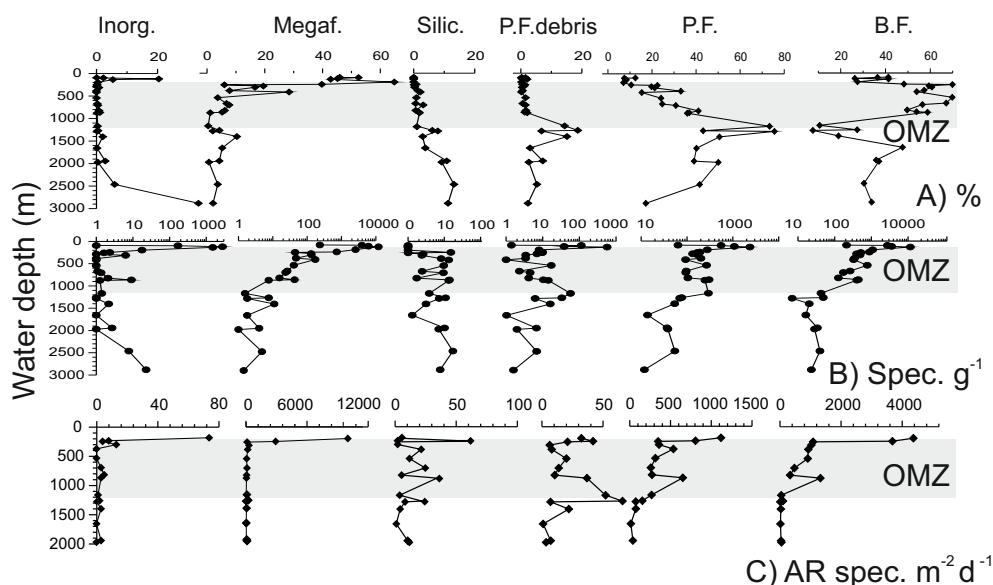


Figure 4. Main components of the coarse fraction ($>150\mu\text{m}$) along the Hab transect (see Fig. 1b, c). Inorg. stands for lithogenic and authigenic particles (quartz, concretions, pyrite, etc.), Megaf. for megafossils (mussels, snails, fish, etc.), Silic. for siliceous biogenic particles (radiolarians, diatoms, sponge spicules), P.F. debris for fragments of planktic foraminifera shells, P.F. for intact planktic foraminifera, and B.F. for benthic foraminifera and fragments. The rows display (A) relative abundance (%), (B) concentration (number of spec. g^{-1}), and (C) accumulation rates (AR) of spec. $\text{m}^{-2} \text{d}^{-1}$ of the six categories. OMZ stands for oxygen minimum zone.

Here we define the onset of the winter high-flux period due to the dramatic shift in bulk flux as high-flux events (HFEs). According to the definition of Schott et al. (2009), that period in the northern Arabian Sea temporally coincides with the late winter NE monsoon period, although the timing of the start of the HFE is slightly different for the two winters sampled.

In EPT2 the HFE shift is observed from collection period 10 to 11 (10 January 1996). In EPT1 an increase is noticed in sampling cup 3, and the strong shift is from cup 4 to cup 5 (20 December 1993). For the deployment of the same year further offshore (WPTs and WPTd were programmed to sample flux simultaneously to EPT1 closer onshore, Table 2), the start of an HFE is fully recorded at the shallow trap WPTs, but occurs one collection period (22 days) later (cup 4). The vertical trap particle flux in the Hab area is about 10 times higher when compared to the open ocean areas of the Arabian Sea (Haake et al., 1993). Moreover, the flux rates and composition within the water column (Fig. 6b), which could be determined only for a limited period of time, agree rather well in dimensions, with the accumulation rates and fractions determined at the seafloor (Fig. 5). Both the water column and seafloor estimates of the bulk flux amount to several thousand $\text{mg m}^{-2} \text{d}^{-1}$, and the CaCO_3 and OC fluxes range from several tens to several hundreds of $\text{mg m}^{-2} \text{d}^{-1}$ (Table 2). An elevated trap flux during and after summer (SW) monsoon (in July/August according to the definition of Schott et al., 2009) could be recorded in EPT2. It is characterized by a higher concentration of OC ($\sim 2\%$), whereas all winter fluxes have

relatively low OC ($\sim 1\%$). An analysis of the winter coarse fraction of EPT2 hints at the origin of the HFE matter: small benthic foraminifera, presumably remobilized from the shelf and upper slope, constitute up to 10% of the foraminiferal flux during the winter season (Schulz et al., 2002).

5 Discussion

Based on our detailed studies of the sediment profiles, the finding of more than one layer leaves some uncertainty on the exact patterns displayed by the sedimentation rates. We described different colors and thicknesses of layers, and observe presumably different event layers deposited one on top of the other at one site (58 KG). This refutes exact synchronism of that marker bed. We suggest that the red and gray layers are almost synchronous. These are separated by 5–10 thin sediment laminae (Staubwasser and Sirocko, 2001), since they were deposited by a similar turbidite or turbid-layer-type gravitational deposition process around $\text{AD } 1905 \pm 10$. We believe that our correlative stratigraphic approach by two event layers may be superior to reconstructions based on individually dated records. Especially those cores from below the OMZ would be at risk of being biased by bioturbation effects. Thick turbidites clearly form the major sediment fraction on the central Makran and clearly contrast with the thin seasonal sediment laminae that characterize the Pakistan Hab (and Indus) margin sections (Bourget et al., 2010; von Rad et al., 1995, their Ormara transect). To this end, the few thick layers in the shallow sediment sections of the Hab area,

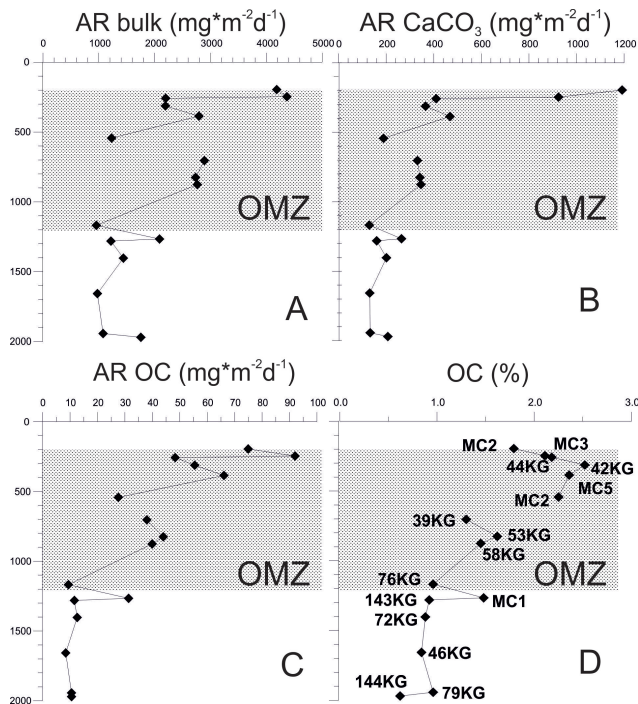


Figure 5. Estimated accumulation rates (AR) of selected bulk parameters vs. water depth. Note that upper stations are on the Indus side, whereas the deeper cores are from the Makran margin. (A) AR bulk, (B) AR CaCO_3 , (C) AR organic carbon OC and (D) sedimentary organic carbon OC (%). OMZ stands for oxygen minimum zone.

sandwiched between laminated sediments, are unique and offer a good opportunity for correlation.

We find a rather low, stable accumulation of organic carbon below the OMZ with an OC AR of only $\sim 10 \text{ mg m}^{-2} \text{ d}^{-1}$. At these sites, we also notice the very low but uniform accumulation of benthic foraminifera. The parallel accumulation rates may document the close relationship between the benthic faunas and available OC (food). This may be valid only for the aerobic fauna. However, approaching the lower margin of the OMZ, significant changes in the faunal composition have been noticed (Schumacher et al., 2007). Zobel (1973) observed a strong reduction of benthic foraminifera at the lower boundary and explained the gap in the study's percentage data (Fig. 4) by a benthic community change between a more aerobic deeper water *Bulimina aculeata* facies and an OMZ *Buliminacea* bio-facies. The high density of benthic foraminifera of $\sim 200\text{--}1000 \text{ spec. m}^{-2} \text{ yr}^{-1}$ (live + dead fauna) in the upper part of the OMZ is in line with the more recent observations showing that benthic foraminifera, as part of the meiofauna, play a central role in OM cycling. In particular, the form *Uvigerina* ex. gr. *semiornata* is present in the upper part of the Pakistan OMZ (Larkin and Gooday, 2009). However, off the Indus margin to the south of Karachi, these authors observe high benthic foraminiferal densities at the deep OMZ, whereas ac-

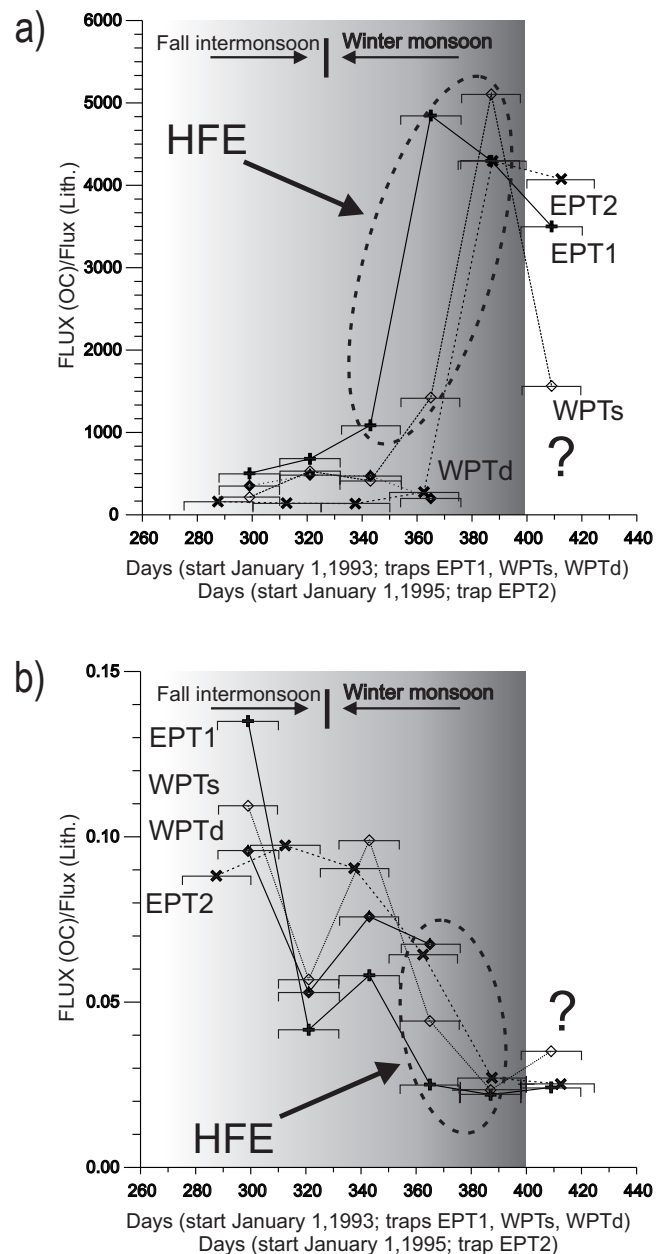


Figure 6. Summarized details of flux recording prior and during the winter high-flux events (HFEs) from the four sediment traps (EPT2, EPT1, WPTs and WPTd). Note that the latter three have synchronous collection periods (see Table 2). (A) Differences in the timing of increasing and peak flux in the shallow traps EPT and WPTs. (B) Composition of settling flux (exemplified by the ratio of OC/lithic). All traps display similar compositions prior to and during the HFEs, culminating in an increase of lithic matter. The shaded area marks the transition from fall intermonsoon (shaded) to winter monsoon (dark gray). The horizontal axis marks days after 1993 for EPT1, WPTs and WPTd, and days after 1995 for EPT2.

cumulation rates in the Hab transect on the eastern Makran show a pattern of decline with water depth, as depicted by most other sediment properties.

Within the OMZ, sediment profiles are largely intact as they lack the smoothing effect of bioturbation. As expected, sedimentation rates are highly variable in an active continental margin setting. It should be mentioned here that neither the OC AR nor the concentration data of our data set can provide us with an estimate of the key parameter, which is organic carbon burial efficiency, to assess any potential preservational effect on OC by the OMZ. Here we provide estimates on the age and porosity (which parallels density) of the sediments, as well as on the O₂ content of the local bottom waters (Table 2), but we miss a measure for diffusion of O₂ into the sediment to comment on whether there are differences in O₂ exposure time. Hartnett et al. (1998) indicated that oxygen exposure time is important, especially in explaining the decline in OC below the OMZ. However, at no site, even with the sediment trap data, can we determine the percentage of OC delivered to the sediments that is actually buried.

As a main finding, our profiles show that the upper boundary of the OMZ is characterized by high OC fluxes at the outer shelf and downslope transport of allochthonous matter. OC AR ($\text{mg m}^{-2} \text{d}^{-1}$) and OC (%) strongly decline from the upper slope ~ 400 m to ~ 800 – 900 m, and again towards the lower margin of the OMZ, where both parameters reach low values at 1200–1300 m and do not decrease further below. Down to 2000 m water depth, OC ARs are $\sim 10 \text{ mg m}^{-2} \text{d}^{-1}$ (~ 1.5 % of the regional primary productivity estimate at the sea surface ($720 \pm 17 \text{ mg OC m}^{-2} \text{d}^{-1}$)). On the outer shelf, at 250 m water depth, that fraction is ~ 10 % (Table 2).

We suggest that the local shelf drainage system of the Hab area may be unique, dominated by a seasonally variable deposition of extremely fine-grained matter downslope. Only very little coarse materials like macrofossil shells or clastic material escape from the shelf (Fig. 4). Our suggestion is in line with the findings to the south of our region, where organic matter on the seafloor of the Indus area is found strongly degraded in the laminated sediments (Woulds and Cowie, 2009; Jeffreys et al., 2009; Vandewiele et al., 2009). However, there is little information on the various sources and pathways of matter. By the comparatively weak bottom currents and the very low ventilation, and by of the local drainage system, the Hab sedimentary environment contrasts with the other highly productive, low-oxygen margin zones of the Arabian Sea basin to the west and to the southeast. For example, OC, C/N, hydrogen index data and mineralogical indicators do not match to the mid-depth oxygen-minimum patterns along the highly productive, steep Oman margin (Pedersen et al. 1992). Attendant downslope reworking and sediment winnowing were found to best explain the OC patterns found there, but sediment laminae today are absent from the Oman margin. As reported previously by Calvert et al. (1995), laminae are also absent, and there is ma-

ior variability in OC content and sediment grain size at any given depth within the OMZ on the Indian margin. However, compared to the eastern Makran, on both margins there is sufficient oxygen to permit some level of bioturbation, even at the OMZ core, and/or insufficient seasonal change in inputs, resulting in the lack of laminae there. The key point that can be inferred from the two studies of Pedersen et al. (1992) and Calvert et al. (1995) is the large range of grain size and OC contents, associated with strong bottom currents on the upper slope and shelf, ultimately resulting in more sandy sediments on the West Indian and Oman margins. Coarse sediments and ripple beds were also clearly observed at the OMZ core off India (von Stackelberg, 1972; Petra Heinz, personal communication, 2014). On the Indus margin, the OC maximum is found at the lower boundary of the OMZ (Cowie et al. 1999), as in many transects off India and Oman. Therefore in these settings, local near-bottom transport and changes in sediment texture are obviously the dominant control on OC distribution, overriding any oxygen effect there. In contrast, our data exhibit an OC maximum near the upper boundary of the OMZ.

The preservation of laminae (Fig. 2) and the completeness of the sediment profiles (Fig. 3) point to a rather stable sedimentary environment and to the reduced importance of near-bottom sediment transport off the Makran coastal zone (Fig. 4). Strong and event-like near-bottom resedimentation events (except the marked clay-silt turbidite) were not recorded from the sediments during the past ~ 100 years in the Hab area and on the upper Indus slope. However, thin silty event deposits of light-gray color are eventually interbedded between the seasonal laminae couplets (see “C layers” in Schulz et al. (1996) and von Rad et al. (2002b); core photos provided as a supplement).

Unique sedimentary conditions may prevail not only across the slope (Fig. 2–5) but also in the water column off the Hab transect. We emphasize that the extremely fine-grained, organic and clastic material resuspended from shallow depths during the winter season is one of the main sedimentary factors that causes the OC maximum near the upper continental margin, and plays an important role for the formation of the Pakistan laminated sediments. Von Rad et al. (2002b) report that there is continuous lamination in the Holocene core 56KA at station 39 KG. For at least the past ~ 5000 years, more than 50 wt% (up to 65 %) of the bulk matter flux was in the clay fraction, with a small median of only $1.8 \mu\text{m}$.

The phenomenon of a high water column flux on the shelf and on the upper margin can also be expected in other margin environments, but has rarely been monitored because of the small number of sediment trap moorings installed at coastal and continental margin sites to record the highly dynamic flux. A good overview of sediment traps issues can be taken from the global trap compilation study of Žaric et al. (2006). Only 1 out of 41 casts was found from a shallow open margin setting with water depths < 1000 m.

For the Pakistan margin, we assume that, due to winter HFE, sediment trap cups and possibly even the funnels were filled with sediment. In both sediment trap time series EPT1 and WPTs of 1993/1994, only the first six cups were filled (Andruleit et al., 2000; Schulz et al., 2002) because trap functions terminated. By the same suspension events traps and finally became clogged (Fig. 6). Whatever the exact reason was for the termination of the records, the three traps (except WPTd) collected a huge amount of suspended matter immediately before they stopped functioning (Fig. 6a). The exact timing of increases in flux is different for the three traps, but it is possible that fluxes followed a temporal and spatial evolution: an HFE in 1993/1994 at EPT1 started in the last weeks of 1993 and was recorded in trap WPTs offshore only in early 1994. We speculate that the HFE of that winter evolved in the coastal and/or shelf margin zones and subsequently spread away from the coast to record the high fluxes 20 km further offshore at WPTs one sampling period later. A very similar winter flux pattern was observed two years later in EPT2. The increase in fluxes recorded in 1995/1996 started relatively late compared to EPT1.

The average flux composition for the winter period was very similar between the more coastal sites and WPTs trap further offshore (Fig. 6b), and the winter flux material strongly resembles that of the sediments (Table 2). We speculate that the upper water column in the late winter season must have been loaded to more than 30 km distance from the shelf edge (2004 m seafloor depth) with a rather uniform sediment suspension. Based on our bulk sediment AR below the traps, we stress that a “normal” flux of sinking matter (as is observed in EPT2 before the HFE) would not be high enough to explain the deposition of several $1000 \text{ mg m}^{-2} \text{ d}^{-1}$ of laminated sediment offshore. As an example, we speculate that the longest time series, EPT2, must have received an HFE up to 20 000 to 30 000 $\text{mg m}^{-2} \text{ d}^{-1}$. This large winter flux is needed to balance the low fluxes of only $\sim 750 \text{ mg m}^{-2} \text{ d}^{-1}$ recorded during spring, summer and fall in order to reach the 2000 to 2500 $\text{mg m}^{-2} \text{ d}^{-1}$ of flux that we reconstructed from sediment stations MC1 and 58 KG below the EPT moorings. However, because of the lack of direct observations, we can only speculate on the temporal and spatial dimensions of the winter resuspension process.

6 Conclusions

1. A quantitative reconstruction of sediment fluxes using a combination of high-quality short sediment cores with sediment trap results leads to a better understanding of the roles of low-oxygen conditions and of the horizontal vs. vertical particle transport across the easternmost part of the upper Makran and the northern section of the Indus margin. As a major finding of the study, we present here precise estimates of the mass accumulation rates and a detailed characterization of the different sediment fractions. We estimate that the total error for the sediment flux reconstructions is $< 20\%$.
2. Profiling of ^{210}Pb , sediment AR determinations and ^{14}C dating has previously been done on the Pakistan, Indus and other margins, though not with the spatial coverage and precision of AR estimates presented in our study. Our studies indicate that the trends in organic carbon concentration seen on the Hab/Makran transects are not typical of other Arabian Sea margins. The identification of an upper-margin organic carbon maximum at $\sim 400 \text{ m}$ is supported by sediment flux estimates spanning the entire OMZ down to 2000 m. These estimates indicate that the main source of the material is from shallow water depths, from the outer shelf and uppermost continental slope, even though the texture of bulk sediments on the slope appears to be extremely fine-grained (clay-sized).
3. From a source-to-sink perspective, our investigations imply that important processes of sediment resuspension and dispersal must take place within the water column. Water column processes dominate over the factors of near-bottom transport and preservation. In the outer shelf area the bulk sediment accumulation rates are $> 4000 \text{ mg m}^{-2} \text{ d}^{-1}$, more than twice the rates at 1000 m water depth. These high rates compare best with those from the sediment traps EPT and WPT during the winter season deployed at only $\sim 600 \text{ m}$ trap depth.
4. The high-flux events (HFE) documented in our traps suggest that large-scale sediment suspensions of $> 5000 \text{ mg m}^{-2} \text{ d}^{-1}$ spread offshore at the upper slope in the (NE) monsoon season. This suggests a strong control by the winter monsoon processes on the sedimentary regime and on the formation of the laminated sediments on the Pakistan margin in the northeastern Arabian Sea.

The Supplement related to this article is available online at [doi:10.5194/bg-11-3107-2014-supplement](https://doi.org/10.5194/bg-11-3107-2014-supplement).

Acknowledgements. The authors thank the editor, Greg Cowie, for helpful comments and the two anonymous reviewers for their thorough and constructive reviews. We thank Birgit Stenschke and Martina Schmidtke for laboratory assistance, Helmut Kawohl and Rainer Goergens for obtaining high-quality sediment cores, and Captain Papenhagen and Captain Kull and their skilled crews for help and good collaboration onboard R.V. *SONNE* and R.V. *METEOR*. The first author wishes to express his sincere thanks to the Hamburg group of marine biogeochemistry – Venu Ittekkot, Andreas Suthhof, Tim Jennerjahn, Jörg Tiemann, Martin Wiesner and Birgit Gaye – for discussions and support. This study was funded by the German Federal Ministry of Education and Research (BMBF), projects 03G0090A (PAKOMIN), 03F0137C (PAKOFLUX) and 03G0806C (CARIMA).

Edited by: G. Cowie

References

- Andrulleit, H. A., von Rad, U., Bruns, A., and Ittekkot, V.: Coccolithophore fluxes from sediment traps in the northeastern Arabian Sea off Pakistan, *Mar. Micropaleontol.*, 38, 285–308, 2000.
- Antoine, D., André, J.-M., and Morel, A.: Oceanic primary production, 2. Estimation at global scale from satellite (coastal zone color scanner) chlorophyll, *Global Biogeochem. Cy.*, 10, 57–69, 1996.
- Berger, W. H. and von Rad, U.: Decadal to millennial cyclicity in varves and turbidites from the Arabian Sea: hypothesis of tidal origin, *Glob. Planet. Change*, 34, 313–325, 2002.
- Bourget, J. Zaragosi, S., Ellouz-Zimmermann, S., Ducassou, E., Prins, M., Garlan, T., Lanfumey, V., Schneider, J.-L., Rouillard, P., and Giraudeau, J.: Highstand vs lowstand turbidite system in the Makran active margin: Imprints if high-frequency external controls on sediment delivery mechanisms to deep water systems, *Mar. Geol.*, 274, 187–208, 2010.
- Calvert, S. E., Pedersen, T. F., Naidu, P. D., and von Stackelberg, U.: On the organic carbon maximum on the continental slope of the eastern Arabian Sea, *J. Mar. Res.*, 53, 269–296, 1995.
- Cowie, G. L., Calvert, S. E., Pedersen, T. F., Schulz, H., and von Rad, U.: Organic content and preservational controls in surficial shelf and slope sediments from the Arabian Sea (Pakistan Margin), *Mar. Geol.*, 161, 23–38, 1999.
- Cowie, G. L.: The biogeochemistry of Arabian Sea surficial sediments: A review of recent studies, *Prog. Oceanogr.*, 65, 260–269, 2005.
- Cowie, G. L. and Levin, L. A.: Benthic biological and biogeochemical patterns and processes across an oxygen minimum zone (Pakistan margin, NE Arabian Sea), *Deep-Sea Res. Pt. II*, 56, 261–270, 2009.
- Cowie, G.L., Mowbray, S., Lewis, M., Matheson, H., and McKenzie, R.: Carbon and nitrogen elemental and stable isotopic compositions of surficial sediments from the Pakistan margin of the Arabian Sea, *Deep-Sea Res. Pt. II*, 56, 271–282, 2009.
- Dietrich, P. G. and Marchig, V.: Sedimentation and early diagenesis in the area of the oxygen minimum off the Indus River (Pakistan, Arabian Sea), *Zentralblatt für Geologie und Paläontologie Teil I*, 1/2, 45–61, 1995.
- Erlenkeuser, H. and Peterstad, K.: Recent sediment accumulation in Skagerrak as depicted by 210-Pb-dating, *Norsk Geologisk Tidsskrift*, 64, 135–152, 1984.
- Haake, B., Ittekkot, V., Ramaswamy, V., Nair, R. R., and Curry, W. B.: Seasonality and interannual variability of particle fluxes to the deep Arabian Sea, *Deep-Sea Res.*, 40, 1323–1344, 1993.
- Hartnett, H. E., Keil, R. G., Hedges, J. I., and Devol, A. H.: Influence of oxygen exposure time on organic carbon preservation in continental margin sediments, *Nature*, 391, 572–574, 1998.
- Helly, J. and Levin, L.: Global distribution of naturally occurring marine hypoxia on continental margins, *Deep-Sea Res. Pt. I* 51, 1159–1168, 2004.
- Jeffreys, R. M., Wolff, G. A. and Cowie, G. L.: Influence of oxygen on heterotrophic reworking of sedimentary lipids at the Pakistan margin, *Deep-Sea Res. Pt. II*, 56, 358–375, 2009.
- Keil, R. G. and Cowie, G. L.: Organic matter preservation through the oxygen minimum zone of the NE Arabian Sea as discerned by organic-mineral interactions, *Chem. Geol.*, 161, 13–22, 1999.
- Larkin, K. E. and Gooday, A. J.: Foraminiferal faunal responses to monsoon-driven changes in organic matter and oxygen availability at 140 and 300m water depth in the NE Arabian Sea. *Deep-Sea Res. Pt. II*, 56, 403–421, 2009.
- Law, G. T. W., Shimmield, T. M., Shimmield, G. B., Cowie, G. L., Breuer, E. R., and Harvey M.: Manganese, iron, and sulphur cycling on the Pakistan margin, *Deep-Sea Res. Pt. II*, 56, 305–323, 2009.
- Limmer, D. R., Köhler, C. M., Hillier, S., Moreton, S. G., Tabrez, A. R., and Clift, P. D.: Chemical weathering and provenance evolution of Holocene-Recent sediments from the Western Indus Shelf, Northern Arabian Sea inferred from physical and mineralogical properties., *Mar. Geol.*, 326–328, 101–115, 2012.
- Lückge, A., Reinhardt, L., Andrulleit, H., Doose-Rolinski, H., von Rad, U., Schulz, H., and Treppke, U.: Formation of varve-like laminae off Pakistan: decoding 5 years of sedimentation, in: *The Tectonic and Climatic Evolution of the Arabian Sea Region*, edited by: Clift, P. D., Kroon, D., Gaedicke, C., and Craig, J., *Geol. Soc. Spec. Publ.*, 195, 421–431, 2002.
- Nair, R. R., Ittekkot, V., Manganini, S. J., Ramaswamy, V., Haake, B., Degens, E. T., Desai, B. N., and Honjo, S.: Increased particle flux to the deep ocean related to monsoons, *Nature*, 338, 749–751, 1989.
- Paropkari, A. L., Babu, C. P. and Mascarenhas, A.: A critical evaluation of depositional parameters controlling the variability of organic carbon in Arabian Sea sediments, *Mar. Geol.*, 107, 213–226, 1992.
- Pedersen, T. F., Shimmield, G. B., and Price, N. B.: Lack of enhanced preservation of organic matter in sediments under the oxygen minimum on the Oman Margin, *Geochim. Cosmochim. Ac.*, 56, 545–551, 1992.
- Piper, D. J. W., and Stow, D. A. V.: *Fine-grained turbidites, in: Cyclic and Event Stratification*, edited by: Einsele, G. and Seilacher, A., New York, Springer Verlag, 360–376, 1991.
- Pollehne, F., Zeitschel, B., and Peinert, R.: Short-term sedimentation patterns in the northern Indian Ocean, *Deep-Sea Res. Pt. II*, 40, 737–752, 1993.
- Ramaswamy, V., Nair, R. R., Manganini, S., Haake, B., and Ittekkot, V.: Lithogenic fluxes to the deep Arabian Sea measured in sediment traps, *Deep-Sea Res.*, 38, 169–184, 1991.

- Rixen, T., Haake, B., and Ittekkot, V.: Sedimentation in the western Arabian Sea, The role of coastal and open-ocean upwelling, *Deep-Sea Res. Pt. II*, 47, 2629–2651, 1999.
- Sarnthein, M., Pflaumann, U., Ross, R., Tiedemann, R., and Winn, K.: Transfer functions to reconstruct ocean paleoproductivity: a comparison, in: *Upwelling Systems, Evolution since the Early Miocene*, edited by: Summerhayes, C. P., Prell, W. L., and Emeis, K.-C., *Geol. Soc. Spec. Publ.*, 64, 411–427, 1992.
- Schott, W., Xie, S.-P., and McCreary, J. P.: Indian Ocean circulation and climate variability, *Rev. Geophys.*, 47, RG1002, doi:10.1029/2007RG000245, 2009.
- Schumacher, S., Jorissen, F., Dissard, D., Larkin, K. E., and Gooday, A. J.: Live (Rose Bengal stained) and dead benthic foraminifera from the oxygen minimum zone of the Pakistan continental margin (Arabian Sea), *Mar. Micropal.*, 62, 45–73, 2007.
- Schultheiss, P. J. and Weaver, P. P. E.: Multi-sensor core logging for science and industry, in: *Proceedings Oceans 92, Mastering the Oceans Through Technology*, 2, 608–613, 1992.
- Schulte, S., Mangelsdorf, K., and Rullkötter, J.: Organic matter preservation on the Pakistan continental margin as revealed by biomarker geochemistry, *Org. Geochem.*, 31, 1005–1022, 2000.
- Schulz, H., von Rad, U., and von Stackelberg, U.: Laminated sediments from the oxygen minimum zone of the northeastern Arabian Sea, in: *Paleoclimatology and Paleoceanography from Laminated Sediments*, edited by: Kemp, A. E. S., *Geol. Soc. Spec. Publ.*, 116, 185–207, 1996.
- Schulz, H., von Rad, U., and Ittekkot, V.: Planktic foraminifera, particle flux and oceanic productivity off Pakistan, NE Arabian Sea: modern analogues and application to the paleorecord, in: *The Tectonic and Climatic Evolution of the Arabian Sea Region*, edited by: Clift, P. D., Kroon, D., Gaedicke, C., and Craig, J., *Geol. Soc. Spec. Publ.*, 195, 499–516, 2002.
- Sirocko F. and Sarnthein, M.: Wind-borne deposits in the northwestern Indian Ocean: record of Holocene sediment versus modern satellite data, edited by: Leinen, M. and Sarnthein, M., *NATO ASI Series C*, 282, 401–433, 1989.
- Staubwasser, M. and Sirocko, F.: On the formation of laminated sediments on the continental margin off Pakistan: the effects of sediment provenance and sediment redistribution, *Mar. Geol.*, 172, 43–56, 2001.
- Suthhof, A., Jennerjahn, T. C., Schäfer, P., and Ittekkot, V.: Nature of organic matter in surface sediments from the Pakistan continental margin and the deep Arabian Sea: amino acids, *Deep-Sea Res. Pt. II*, 47, 329–351, 2000.
- Thiede, J., Suess, E., and Müller, P. J.: Late Quaternary Fluxes of Major Sediment Components to the Sea Floor at the Northwest African Continental Slope, in: *Geology of the Northwest African Continental Margin*, edited by: von Rad, U., Hinz, K., Sarnthein, M., and Seibold, E., Springer Verlag, 605–631, 1982.
- van der Weijden, C. H., Reichart, G. J., and Visser, H. J.: Enhanced preservation of organic matter in sediments deposited within the oxygen-minimum zone in the northeastern Arabian Sea, *Deep-Sea Res.*, 46, 807–830, 1999.
- Vandewiele, S., Cowie, G. L., Soetaert, K., and Middelburg, J. J.: Amino acid biogeochemistry and organic matter degradation state across the Pakistan margin oxygen minimum zone, *Deep-Sea Res. Pt. II*, 56, 376–392, 2009.
- von Rad, U., Schulz, H., and SONNE 90 Scientific Party: Sampling the Oxygen Minimum Zone off Pakistan: Glacial/Interglacial variations of anoxia and productivity, *Mar. Geol.*, 125, 7–19, 1995.
- von Rad, U., Schaaf, M., Michels, K. H., Schulz, H., Berger, W. H., and Sirocko, F.: A 5000-year record of climate change in varved sediments from the Oxygen Minimum Zone off Pakistan, Northeastern Arabian Sea, *Quat. Res.*, 51, 39–53, 1999.
- von Rad, U., Deslisle, G., and Lückge, A.: On the formation of laminated sediments on the continental margin of Pakistan – Comment, *Mar. Geol.*, 192, 425–429, 2002a.
- von Rad, U., Ali Khan, A., Berger, W.H., Rammlmair, D., and Treppke, U.: Varves, turbidites and cycles in upper Holocene sediments (Makran slope, northern Arabian Sea), in: *The Tectonic and Climatic Evolution of the Arabian Sea Region*, edited by: Clift, P. D., Kroon, D., Gaedicke, C., and Craig, J., *Geol. Soc. Spec. Publ.* 195, 387–406, 2002b.
- von Stackelberg, U.: Faziesverteilung in Sedimenten des indisch-pakistanischen Kontinentalrandes (Arabisches Meer), “Meteor”-Forsch.-Ergebnisse, Reihe C, 9, 1–73, 1972.
- Weber, M. E., Niessen, F., Kuhn, G., and Wiedecke, M.: Calibration and application of marine sedimentary physical properties using a multi-sensor core logger, *Mar. Geol.*, 136, 151–172, 1997.
- Wiggert, J. D., Hood, R. R., Banse, K., and Kindle, J. C.: Monsoon-driven biogeochemical processes in the Arabian Sea, *Prog. Oceanogr.*, 65, 176–213, 2005.
- Woulds, C. and Cowie, G. L.: Sedimentary pigments on the Pakistan margin: Controlling factors and organic matter dynamics, *Deep-Sea Res. Pt. II*, 56, 347–357, 2009.
- Žaric, S., Schulz, M., and Mulitza, S.: Global prediction of planktic foraminiferal fluxes from hydrographic and productivity data, *Biogeosciences*, 3, 187–207, doi:10.5194/bg-3-187-2006, 2006.
- Zobel, B.: Biostratigraphische Untersuchungen an Sedimenten des indisch-pakistanischen Kontinentalrandes (Arabisches Meer), “Meteor” Forsch. Ergebnisse, Reihe C, 12, 9–73, 1973.